

## Performance analysis of the SO/PHI software framework for on-board data reduction

K. Albert,<sup>1</sup> J. Hirzberger,<sup>1</sup> D. Busse,<sup>1</sup> J. Blanco Rodríguez,<sup>2</sup>, J. S. Castellanos Duran<sup>1</sup>, J. P. Cobos Carrascosa,<sup>3</sup> B. Fiethe,<sup>4</sup> A. Gandorfer,<sup>1</sup> Y. Guan,<sup>4</sup> M. Kolleck,<sup>1</sup> T. Lange,<sup>4</sup> H. Michalik,<sup>4</sup> S. K. Solanki,<sup>1</sup> J. C. del Toro Iniesta,<sup>3</sup> and J. Woch<sup>1</sup>

<sup>1</sup>*Max Planck Institute for Solar System Research, Göttingen, Germany;*  
*albert@mps.mpg.de ,*

<sup>2</sup>*Universidad de Valencia, Paterna (Valencia), Spain*

<sup>3</sup>*Instituto de Astrofísica de Andalucía (IAA - CSIC), Granada, Spain,*

<sup>4</sup>*Institute of Computer and Network Engineering at the TU Braunschweig, Braunschweig, Germany*

**Abstract.** The Polarimetric and Helioseismic Imager (PHI) is the first deep-space solar spectropolarimeter, on-board the Solar Orbiter (SO). It faces: stringent requirements on its science data accuracy, dynamic environments and severe limitations on telemetry volume. SO/PHI overcomes these limitations through on-board instrument calibration and science data analysis, using dedicated firmware in reconfigurable FPGA-s. This contribution analyses the accuracy of a data processing pipeline by comparing the results obtained with a SO/PHI model to a reference by a ground computer. The results show that for the analysed pipeline the error introduced by the firmware implementation is well below the requirements, leaving a large margin for other error sources.

### 1. Introduction

The Polarimetric and Helioseismic Imager (PHI) is one of ten instruments to be carried around the Sun by Solar Orbiter (SO) (Müller et al. 2013). SO/PHI (Solanki et al. 2018), is an imaging spectropolarimeter, probing the photospheric FeI 6173 Å absorption line.

SO/PHI records data in five dimensions: time series of data sets containing 2048 x 2048 pixel images of the Sun sampling the target absorption line at six wavelengths, recording four different polarisation states at each wavelength. These polarisation states contain linear combinations of the Stokes parameters (**S**), a formalism to describe the polarisation of light in terms of four ideal filters, denoted *I*, *Q*, *U* and *V*. To arrive to the Stokes images (the input for scientific analysis), the recorded polarisation states are demodulated with the Demodulation Matrix (**D**). These images, complemented with a wavelength dimension, encode the magnetic field vector at the mean formation height of the absorption line and the line of sight (LOS) due to the Zeeman and Doppler effects. Arriving to these quantities is possible by the inversion of the Radiative Transfer Equation (RTE). See del Toro Iniesta (2003) for more on spectropolarimetry.

SO/PHI is the first spectropolarimeter on a deep space mission, facing unprecedented dynamic environment and telemetry limitations. These challenges are met with a full and autonomous on-board data analysis system: determines the instrument char-

acteristics, corrects the data with the measured calibration data, then derives the targeted physical parameters. This system is implemented on a data processing unit with two Field Programmable Gate Arrays (FPGAs), reconfigured in flight to perform image processing functions (Fiethe et al. 2012; Lange et al. 2017), and a microprocessor running a data processing framework that combines these functions into pipelines (Albert et al. 2018). This contribution analyses errors induced by the on-board processing.

## 2. The on-board data analysis software

The science data processing, one of the two on-board data processing types, comprises of data preprocessing (correcting the data for instrumental effects and polarimetric demodulation) and of the RTE inversion. The preprocessing primarily corrects the images for the dark field and the flat field of the instrument, and does the polarimetric demodulation. It may have additional steps (e.g. spatial cropping or deconvolution from point spread function), depending on science case and the instrument parameters determined at instrument commissioning. The RTE inversion transforms the 24-image spectropolarimetric dataset into 5 images of interest: azimuth, elevation and magnitude of the magnetic field vector, the LOS velocity and the total intensity at continuum wavelength. See Cobos Carrascosa et al. (2016) for details on SO/PHI's RTE inversion.

To save FPGA resources, in the preprocessing functions fixed point number representation is used on 24.8 bits, while the RTE inversion is done in 32 bits floating point. The most basic preprocessing pipeline for a data set from an imaging spectropolarimeter contains dark and flat field correction and polarimetric demodulation:

$$\mathbf{S}_\lambda(x, y) = \mathbf{D}(x, y) \cdot [(\mathbf{I}_\lambda^{obs}(x, y) - I^{dark}(x, y)) / I^{flat}(x, y)], \quad (1)$$

where "." denotes matrix multiplication,  $\lambda$  marks wavelength dependence,  $x$  and  $y$  are spatial dimensions. The Stokes parameters is  $\mathbf{S} = [I, Q, U, V]^T$ .  $\mathbf{D}$  is the  $4 \times 4$  Demodulation Matrix,  $\mathbf{I}^{obs}$  is the observed data in the four modulation states.  $I^{dark}$  is the dark field of the sensor, and  $I^{flat}$  is the flat field of the telescope, neither depending on wavelengths and modulation states (may change for the flat field after commissioning).

To implement equation 2, four blocks are used, combined into a pipeline (see figure 1). The full well in the raw data is always integer, represented on 14.8 bits. As the exposure time is calibrated to fill a predefined percentage of the full well, the recorded data is ideally represented. To process the data at the highest possible resolution, we shift the pixels of these images to the top of the full range ( $\cdot 2^9$ ), arriving to 23.8 bits (one bit is sign). This representation is the block interface, however some blocks re-scale the images to optimise the output accuracy (e.g. at division).

We quantify the errors introduced through on-board processing by running the pipeline on a representative SO/PHI model (using fixed point) and on ground (using floating point in Python). The test data is from the Solar Dynamics Observatory / Helioseismic and Magnetic Imager (Schou et al. 2012), run through the SO/PHI instrument simulator software, SOPHISM (Blanco Rodríguez et al. 2018). This data is modulated into intensities measured by the instrument, then degraded with the ground-measured flat and dark field of the SO/PHI flight model (also used for correction by the pipeline). We compare the results of the Flat fielding, and of the Polarimetric demodulation. The RTE inversion is done on a ground computer, with the He-Line Information Extractor inversion code [HELIx<sup>+</sup>] (Lagg et al. 2004). [HELIx<sup>+</sup>] assumes a Milne-Eddington approximation of the atmosphere, the same as SO/PHI's inversion. The differences in the

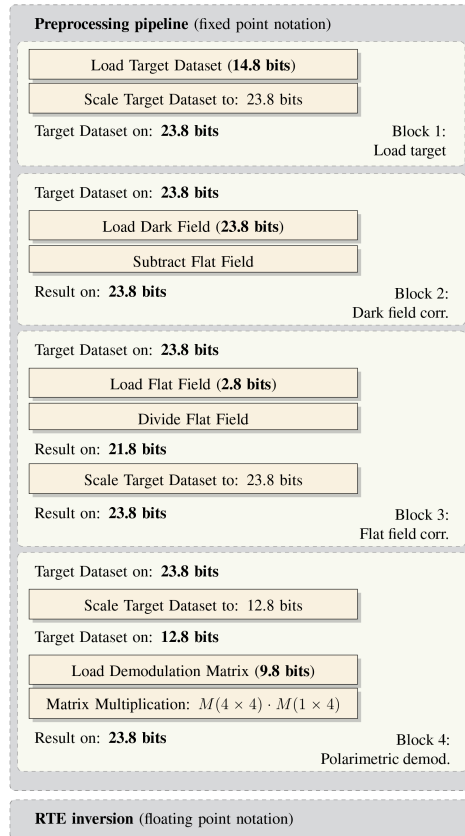


Figure 1. The studied pipeline. The preprocessing controls accuracy by scaling.

RTE inversion results of the two data sets (from SO/PHI and from ground) indicate the error to be expected in the physical parameters, however, it is not an exact measure.

### 3. Results

The flat field division errors are below  $10^{-3}$  (compared to the reference results), apart from a few small outliers in the divisor, with Root Mean Square (RMS) around  $5 \cdot 10^{-5}$ .

SO/PHI requires the accuracy of the polarisation signals (i.e.  $\mathbf{S}/I_{\lambda=\text{continuum}}$ ) to be better than  $10^{-3}$ . Figure 2 shows the error histogram at  $\lambda_3$ . All pixels comply, with their RMS in the order of  $10^{-6}$ , leaving a large margin for other error sources. The errors decrease from the previous step due to the nature of polarimetry, which calculates the difference between signals, partially cancelling previous errors. Furthermore, the error in  $Q/I_{cont}$  is larger than in the rest of the Stokes images, due to a small term in  $\mathbf{D}$ .

The comparison of the physical parameters serves only as indication. The magnetic field strength error RMS is 0.14 G (inside the sunspot). The state of the art measurement precision is cca. 20 G. In the magnetic field azimuth and inclination commonly a few degrees accuracy is expected, met with RMS of  $1.9^\circ$  for the azimuth,  $0.039^\circ$  for the inclination. The LOS velocity is considered accurate to cca.  $10 \text{ ms}^{-1}$  in current measurements, met with  $7 \cdot 10^{-3} \text{ ms}^{-1}$  RMS (calculated in the whole solar disk).

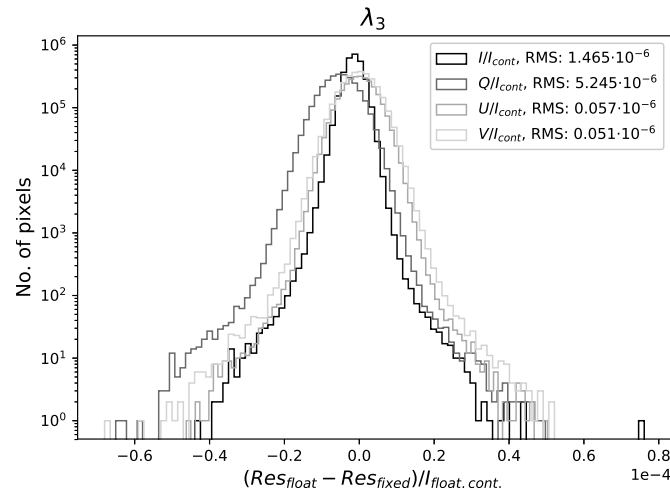


Figure 2. Histogram of polarimetric errors, showing requirement compliance.

#### 4. Conclusions

SO/PHI is the first instrument of its kind to perform on-board data analysis, including data preprocessing and the inversion of the RTE. These steps use computationally demanding image processing functions, implemented on FPGAs. The fixed point number representation in the on-board preprocessing was motivated by resource limitations.

The errors induced by the preprocessing conform with requirements, with a good margin for other sources. This is achieved by keeping full control over data accuracy, a significant overhead. Errors in Fourier domain processing are being analysed currently.

#### Acknowledgements

Workframe: International Max Planck Research School (IMPRS) for Solar System Science. Solar Orbiter: ESA, NASA. Support grants: DLR 50 OT 1201, Spanish Research Agency ESP2016-77548-C5, European FEDER. Data: NASA/SDO HMI science team.

#### References

- Albert, K., et al. 2018, in Proc. SPIE, vol. 707, 10707
- Blanco Rodríguez, J., et al. 2018, The Astrophysical Journal Supplement Series, 237, 35
- Cobos Carrascosa, J. P., et al. 2016, in Proc. SPIE, vol. 9913, 9913
- del Toro Iniesta, J. C. 2003, Introduction to spectropolarimetry (Cambridge university press)
- Fiethe, B., Bubenhausen, F., Lange, T., Michalik, H., Michel, H., Woch, J., & Hirzberger, J. 2012, in NASA/ESA Conference on Adaptive Hardware and Systems, 31
- Lagg, A., Woch, J., Krupp, N., & Solanki, S. K. 2004, Astronomy and Astrophysics, 414, 1109
- Lange, T., Fiethe, B., Michel, H., Michalik, H., Albert, K., & Hirzberger, J. 2017, in NASA/ESA Conference on Adaptive Hardware and Systems, 186
- Müller, D., et al. 2013, Solar Physics, 285, 25
- Schou, J., et al. 2012, Solar Physics, 275, 229
- Solanki, S., et al. 2018, Submitted to Astronomy and Astrophysics